Dispensing Nano-Pico Droplets of Ferrofluids

A Thesis

Presented to

The Faculty of the Department of Mechanical Engineering

University of Houston

In Partial Fulfillment

Of the Requirement for the Degree

Master of Science

In Mechanical Engineering

By

Peyman Irajizad

December 2016

Dispensing Nano-Pico Droplets of Ferrofluids

Peyman Irajizad

Approved:

Chair of the Committee
Hadi Ghasemi, Bill D. Cook Assistance Professor,
Mechanical Engineering

Committee Members:

Di Yang, Assistant Professor,
Mechanical Engineering

Haleh Ardebili, Bill D. Cook Associate Professor,
Mechanical Engineering and Materials Program

Suresh K. Khator, Associate Dean,
Cullen College of Engineering

Pradeep Sharma, Professor and Chair,
Mechanical Engineering

Acknowledgment

Firstly, I would like to express my sincere gratitude to my advisor, Professor Ghasemi for the continuous support of my Masters study, for his patience, motivation, and immense knowledge. His guidance helped me in all the time of research and writing of this thesis. I could not have imagined having a better advisor and mentor for my thesis.

In the committee I would like thank Professors Ardebili and Yang for their responses to all my emails (late and early) and for accepting to be in my thesis committee.

To my family, I thank my wife and my parents for supporting me emotionally and mentally when I got stuck or needed reclusion.

I also acknowledge University of Houston for their support for this project.

Without the support, encouragement, and dedication to assist me, this dissertation would not have been possible.

Dispensing Nano-Pico Droplets of Ferrofluid

An Abstract

of a

A thesis

Presented to

The Faculty of the Department of Mechanical Engineering

University of Houston

In Partial Fulfillment

Of the Requirements for the Degree

Master of Science

In Mechanical Engineering

By

Peyman Irajizad

December 2016

Abstract

Dispensing miniature volumes of a ferrofluid is of fundamental and practical importance for diverse applications ranging from biomedical devices, optics, and self-assembly of materials. Current dispensing systems are based on microfluidics flow-focusing approaches or acoustic actuation requiring complicated structures. A simple method is presented to continuously dispense the miniature droplets from a ferrofluid reservoir. Once a jet of the ferrofluid is subjected to a constrained flux through a membrane and an inhomogeneous magnetic field, the jet experiences a curvature-driven instability and transforms to a droplet. Ferrofluid droplets in the range of 0.1–1000 nl are dispensed with tunable dispensing frequencies. A model was developed, which predicts the dispensed volume of the ferrofluid droplets with an excellent agreement with the measurements.

Table of Contents

Acknowledgment v

Abstract vii

Table of Contents viii

List of Figures ix

Nomenclature x

1. Introduction 1

2. Experimental platform and results 2

3. Theoretical model 7

4. Conclusions 14

References 15

List of Figures

Figure 1. Schematic of the experimental platform.....3

Figure 2. A ferrofluid reservoir is exposed to magnetic field.....4

Figure 3. The measured volumes of the ferrofluid droplets.....5

Figure 4. Dispensing frequencies of the generated droplets.....6

Figure 5. The predicted critical radii for rupture of the ferrofluid jet.....11

Figure 6. Temporal radius of thinning jet at the rupture.....12

Figure 7. The predicted dispensed volume of the ferrofluid.....13

Nomenclature

Term	Definition
PCTE	Polycarbonate
PTFE	Polytetrafluoroethylene
CA	Contact angle

1. Introduction

Ferrofluids are fluids with properties tailored on the nanometer scale.[1] They consist of single domain magnetic nano-particles dispersed in a liquid carrier. As their properties are remotely tunable by a magnetic field, the ferrofluids are exploited in a broad range of disciplines[2,3] including magnetic drug targeting,[4] cancer treatment by magnetic hyperthermia,[5] contrast agent in magnetic resonance imaging (MRI),[6] magnetic-capillary self-assembly,[7,8] optics,[9] sensors,[10] and mechanical sealing and acoustic.[11] In these implementations, dispensing a small volume of fluid is in demand.[12] Current systems for dispensing the ferrofluid droplets at small volumes are mostly based on the microfluidics flow-focusing approaches,[13,14] induced acoustic actuation,[15] or conventional injection systems, requiring complicated dispensing systems.

Here, we show a facile approach to continuously dispense nano/pico liter ferrofluid droplets from a ferrofluid reservoir. In this approach, the ferrofluid reservoir is covered with a membrane. An imposed inhomogeneous localized magnetic field to the reservoir generates a continuous jet of the ferrofluid. Once the jet flows through the membrane, the jet experiences a constrained flux. The combination of constrained flux and inhomogeneous magnetic force results in the thinning of the ferrofluid jet. As the ferrofluid jet becomes thin enough, it goes through a capillary induced instability and breaks into a droplet. Volumes of the dispensed droplets are tuned in the range of 0.1–1000 nl by the induced magnetic field and hydraulic resistance of the membrane. The developed approach promises a simple route to dispense a miniature volume of the ferrofluid with no complex injection systems.

2. Experimental platform and results

The experimental platform for dispensing the ferrofluid droplets is shown in **Fig. 1**. A ferrofluid reservoir is covered with a membrane and is subjected to a localized magnetic field. The ferrofluid, herein, is an oil-based ferrofluid (EMG909, Ferrotec, Inc.). Two types of membrane, Polycarbonate (PCTE) and Polytetrafluoroethylene (PTFE), with a range of pore sizes are studied in this work. The magnetic field is localized at the center of the membrane to suppress formation of simultaneous droplets. Dynamics of the ferrofluid droplets is visualized with a high-speed camera (Phantom V711, vision research). Since the generated droplets are small, we coupled macro lens (MP-E65mm, Canon) or a Nikon microscope (ECLIPSE LV100ND) with the high-speed camera to visualize the dynamics of the ferrofluid droplets.

In the absence of a membrane, if the ferrofluid reservoir is subjected to a magnetic force lower than a threshold value, the ferrofluid-air interface adopts a hump shape to satisfy the static fluid equation, which includes magnetic, gravitational, and surface tension forces.[16] As the magnetic force exceeds this threshold value, the static hump interface transforms to a jet of the ferrofluid, as shown in **Fig. 2(a)**. In jet regime of the magnetic force, if a membrane is introduced on top of the ferrofluid reservoir, the continuous jet of the ferrofluid ruptures and the jet transforms to a droplet, as shown by the time steps in **Figs. 2(b)–2(h)** (Multimedia view).

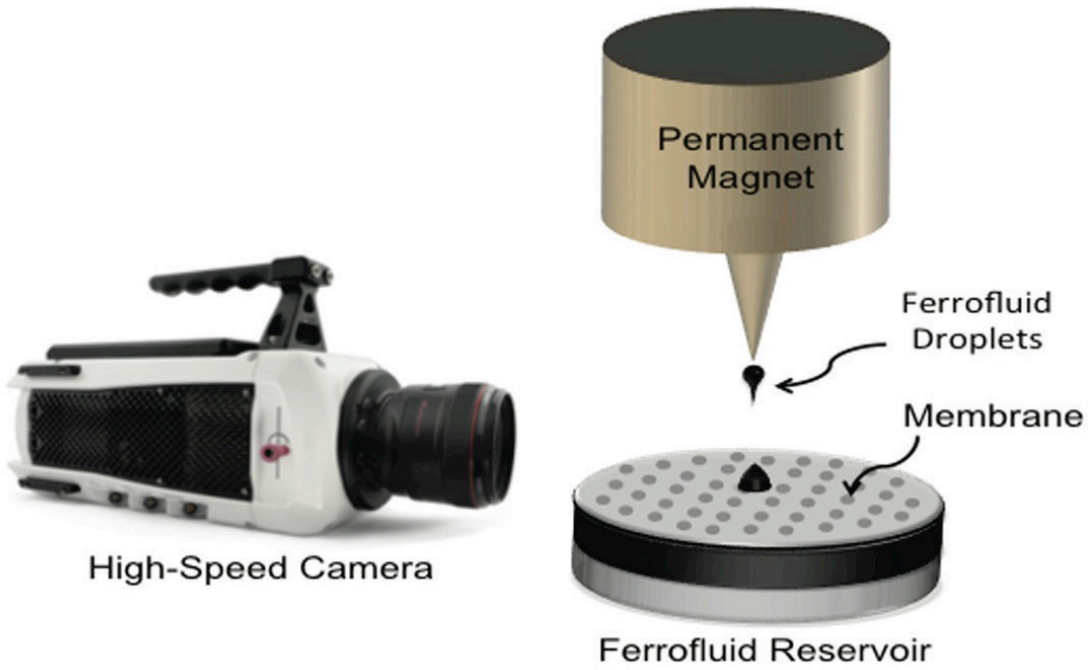

Figure 1. Schematic of the experimental platform. The experimental apparatus comprises a ferrofluid reservoir, a porous membrane, and a localized permanent magnet. The ferrofluid is an oil-based ferrofluid. The localization of magnetic field suppresses the formation of simultaneous droplets.

Although the formation of only one droplet is shown in **Figs. 2(b)–2(h)**, dispensing of the droplets continues indefinitely (see **Fig. 2**, Multimedia view). The jet of the ferrofluid, which leaves the membrane, accelerates in the inhomogeneous magnetic field toward the magnet. As the jet-front moves toward the magnet, the jet progressively thins down because of the constrained flow rate through the membrane and the inhomogeneous magnetic field. At a critical radius, necking occurs in the jet resulting in the back flow of ferrofluid to the reservoir and rupture of the ferrofluid jet. We divided the droplet dispensing process into two regimes: (I) the time interval in which the jet-front moves from the reservoir to the magnet, t_1 (i.e., **Figs. 2(b)–2(d)**). (II) The time interval after regime (I) till rupture of the ferrofluid jet, t_2 (i.e., **Figs. 2(e)–2(g)**).

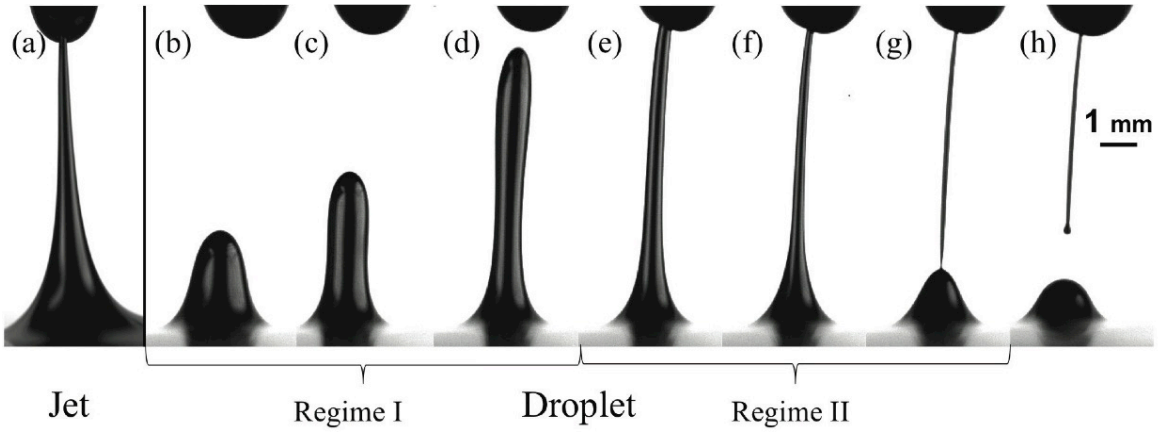

Figure 2. A ferrofluid reservoir is exposed to a localized inhomogeneous magnetic field. (a) A continuous jet is formed in the absence of a membrane and (b)–(g) a jet transforms to a droplet. The membrane in this figure is a polycarbonate membrane (PCTE) with 10 $\boldsymbol{\mu m}$ pore sizes.

Volume of the ferrofluid droplets is determined by summation of dispensed volumes in regimes (I) and (II). We measured the dispensed volume in regime (I) through image analysis of the ferrofluid jet just before touching the magnet. The volume in regime (II) is determined through the integration of mass flux through the membrane in the measured time interval of t_2. We noticed that in all the experiments, the dispensed volume in regime (II) is less than 20% of the total dispensed volume of the ferrofluid. The measured dispensed volumes of the ferrofluid are shown in **Fig. 3** as a function of the imposed magnetic field at the membrane surface. In general, at a given magnetic field, a membrane with smaller pore size (higher hydraulic resistance) generates smaller dispensed volume of the ferrofluid. Since the stiffness of PCTE membrane is low, deformation of the membrane occurs at high magnetic fields ($\geq 100\, mT$). For this reason, we used PTFE membrane for the experiments at these high magnetic fields. Through the developed approach, we dispensed the ferrofluid droplets in the range of 0.1–1000 nl.

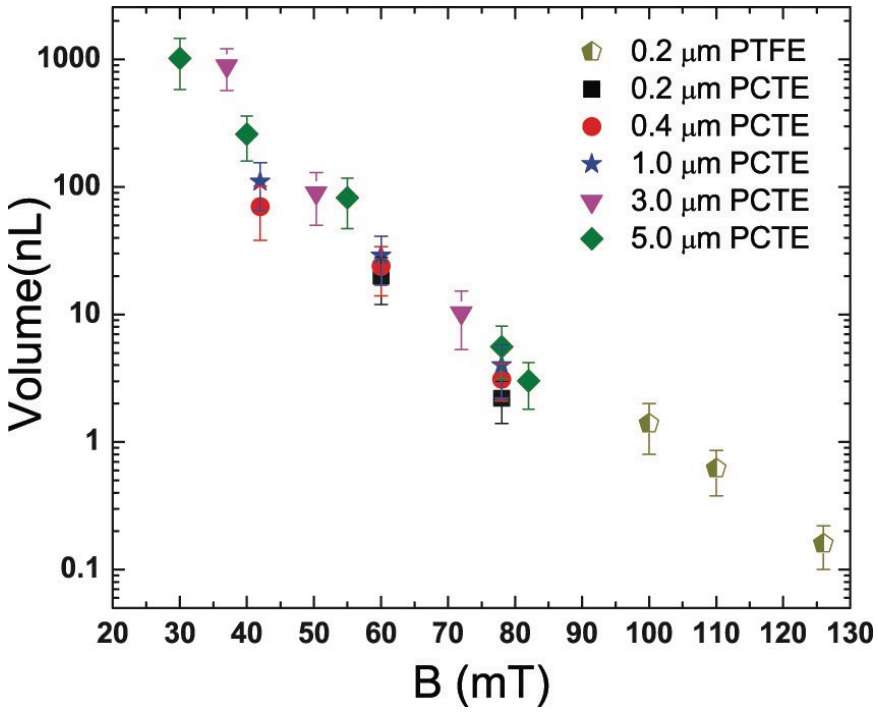

Figure 3. The measured volumes of the ferrofluid droplets are shown as a function of the localized magnetic field at the membrane surface. High hydraulic resistance of membrane and high magnetic field lead to smaller volume of ferrofluid. Volume of the generated droplets varies between 0.1 and 1000 nl.

We emphasize that dispensing lower volume of the ferrofluids can be achieved by a higher magnetic field or utilization of membranes with higher hydraulic resistance. Furthermore, we measured dispensing frequency of these droplets by various membranes as shown in **Fig. 4**.

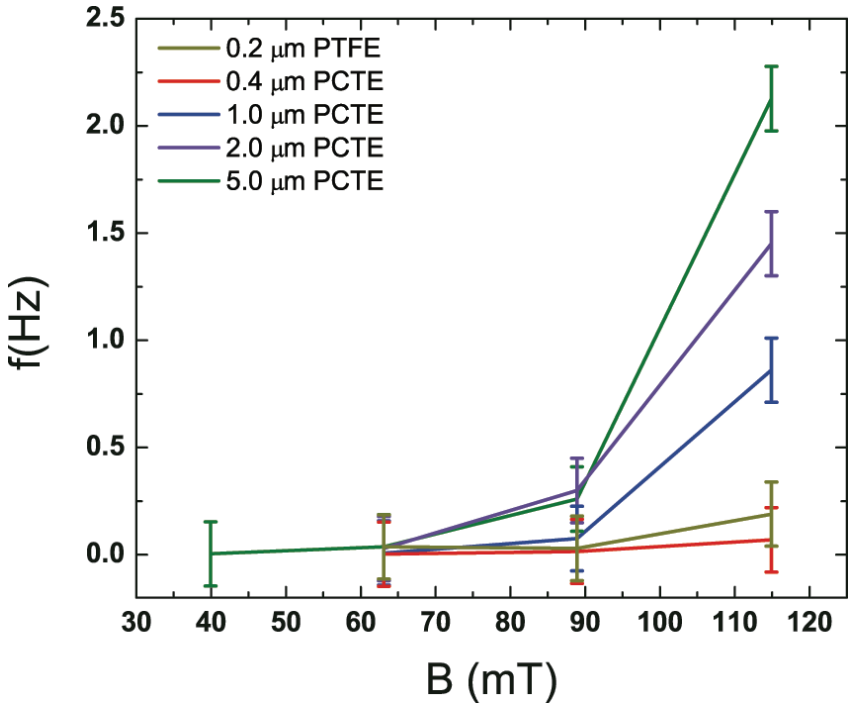

Figure 4. Dispensing frequencies of the generated droplets are shown as a function of the localized magnetic field at the membrane surface for various types of membrane. This frequency is tunable by the imposed magnetic force and hydraulic resistance of the membranes.

3. Theoretical model

In the next step, we developed a model to predict volume of the dispensed ferrofluid droplets. The fluid flow through a membrane is characterized by Darcy's law written as

$$0 = -\boldsymbol{\nabla} p - \beta \boldsymbol{q} + \rho \boldsymbol{g} + \boldsymbol{f}_m, \qquad (1)$$

where p denotes the hydrodynamic pressure, $\beta \left(= \frac{\eta}{K}\right)$ is the ratio of fluid viscosity to inverse of hydraulic resistance of membrane, $\boldsymbol{q}$ is the local average fluid velocity, ρ is the fluid density, $\boldsymbol{g}$ is the gravitational acceleration, and $\boldsymbol{f}_m$ is the magnetic body force density. The magnetic force density is a function of the ferrofluid susceptibility and the imposed magnetic field and is given by

$$\boldsymbol{f}_m = \mu_0 \chi \boldsymbol{\nabla} \mathbf{H^2}, \qquad (2)$$

where μ_0 denotes vacuum magnetic permeability, χ is the susceptibility of the ferrofluid, and $\mathbf{H}$ is the magnetic field. The imposed magnetic field is higher than the saturation magnetization of the studied ferrofluid (22 mT), thereby the expression of magnetic force density is simplified to $\boldsymbol{f}_m = \mu_0 \mathbf{M} \boldsymbol{\nabla} \mathbf{H}$, where $\mathbf{M}$ $(= \chi \boldsymbol{H})$ (denotes magnetization of the ferrofluid. Integration of q over the base area of the jet, A, provides volumetric flux of the ferrofluid through the membrane,Q_m. For a ferrofluid jet flowing through a thin membrane (thickness of 10 μm), contribution of hydrodynamic pressure and the gravitational force are negligible thereby $Q_m = \iint \beta^{-1} \boldsymbol{f}_m dA$. Thus, the dispensed volume of the ferrofluid droplet is written as

$$V_d = \int_0^t Q_m dt, \tag{3}$$

where t denotes the time interval of the ferrofluid flow through the membrane before rupture. We determined dispensed volumes in regime (I), V_1 and in regime (II), V_2 separately through Eq. (3) and summed together to predict the total volume of the dispensed ferrofluid droplets.

The magnetic field is expressed as $\boldsymbol{H} = \boldsymbol{B}{\mu_0}^{-1}(1+\chi)^{-1}$, where $\boldsymbol{B}$ denotes induction magnetic field. We simulated the induction magnetic field of the considered permanent magnet by COMSOL. The simulations suggest that the gradient of induction magnetic field in other coordinates is much smaller than in the z coordinate, and consequently, are neglected. The spatial dependence of the induction magnetic field, $\boldsymbol{B}$, is measured by a Teslameter (HT20 SMA105010) and is well described by

$$B = (\alpha \ln(d - z) + \beta), \tag{4}$$

where d denotes the distance between the reservoir and the magnet, and α and β are the fitting coefficients ($\alpha = -0.028$ and $\beta = -0.1069$). The momentum conservation for the ferrofluid neglecting viscous and convective terms is given by

$$\rho \frac{\partial \boldsymbol{v}(x,t)}{\partial t} = -\boldsymbol{\nabla} p + \rho \boldsymbol{g} + \boldsymbol{f}_m, \tag{5}$$

where $\boldsymbol{v}(x,t)$ denotes the velocity of the ferrofluid. Thus, the motion of the ferrofluid is adequately described as a function of z by Eqs. (2), (4), and (5). We integrate Eq. (5) to determine the velocity of the jet-front in regime (I), $\int_0^d \frac{\partial v(x,t)}{\partial t} dz = \int_{v_0}^{v(t)} v dv$, where v_0

denotes the velocity of the ferrofluid at the membrane surface and is equal to $\beta^{-1} = \boldsymbol{f}_m$. Given the velocity of jet-front, the time interval of regime (I) is determined as $t_1 = \int_0^d v^{-1} dz$. The determined time interval provides the boundary of the integral in Eq. (3) to predict the dispensed volume in regime (I). We emphasize that only properties of the ferrofluid, hydraulic resistance of membrane, and the applied magnetic field are required to predict V_1.

The dispensed volume of the ferrofluid in regime (II), V_2, is determined through Eq. (3) and t_2. One needs to calculate the dynamics of jet necking, $r(t)$, and the rupture radius, r_c, to extract value of t_2. As discussed, the limited flux through the membrane and the induced inhomogeneous magnetic field results in the thinning of the ferrofluid jet. For a thin jet of the ferrofluid, the pressure of ferrofluid is dominantly influenced by Laplace forces rather than gravitational and magnetic forces. This induced pressure by curvature of the ferrofluid jet results in the back flow to the reservoir and thereby necking of the jet. We determined the critical radius for necking of the ferrofluid jet through the integration of Eq. (5). At the critical radius, r_c, velocity of the ferrofluid at the necking point becomes zero and thereby

$$\kappa\gamma - \rho g z + \mu_0 M H = 0, \qquad (6)$$

where $\kappa(=\frac{1}{r_c})$ denotes the curvature of the ferrofluid jet. Note that the first curvature of the ferrofluid-air interface is so small and negligible. Equation (6) is solved to determine r_c for rupture of the ferrofluid jet. The predicted values of r_c for one representative

membrane are compared with the measured experimental values of r_c in **Fig. 5**. The comparison between the prediction and measurements is excellent for all the experiments.

Once the critical radius of the rupture is determined, the temporal dependence of jet's radius at the necking coordinate is required to determine the dispensed volume in regime (II), V_2. The conservation of mass requires that mass flux, $Q_m = \pi r^2(t)\boldsymbol{v}(z,t) = cst$. The derivative of this equation with respect to time is written as

$$\rho \frac{\partial \boldsymbol{v}}{\partial t} = \left(\frac{-2\rho Q_m}{\pi}\right) r(t)^{-3} \frac{\partial r}{\partial t}, \tag{7}$$

where $r(t)$ denotes temporal radius of the ferrofluid jet at the rupture coordinate, **Fig. 5(a)**. We combined the conservation of mass, Eq. (7), and the conservation of momentum, Eq. (5), to derive the governing equation of jet's radius

$$r(t)^{-3} \frac{\partial r}{\partial t} = \frac{\gamma \pi}{2Q_m \rho z_0}\left(\frac{1}{r(t)}\right) + \frac{\pi}{2Q_m}(g - \frac{f_m}{\rho}), \tag{8}$$

where z_0 denotes the vertical coordinate at the rupture point (see **Fig. 5(a)**).

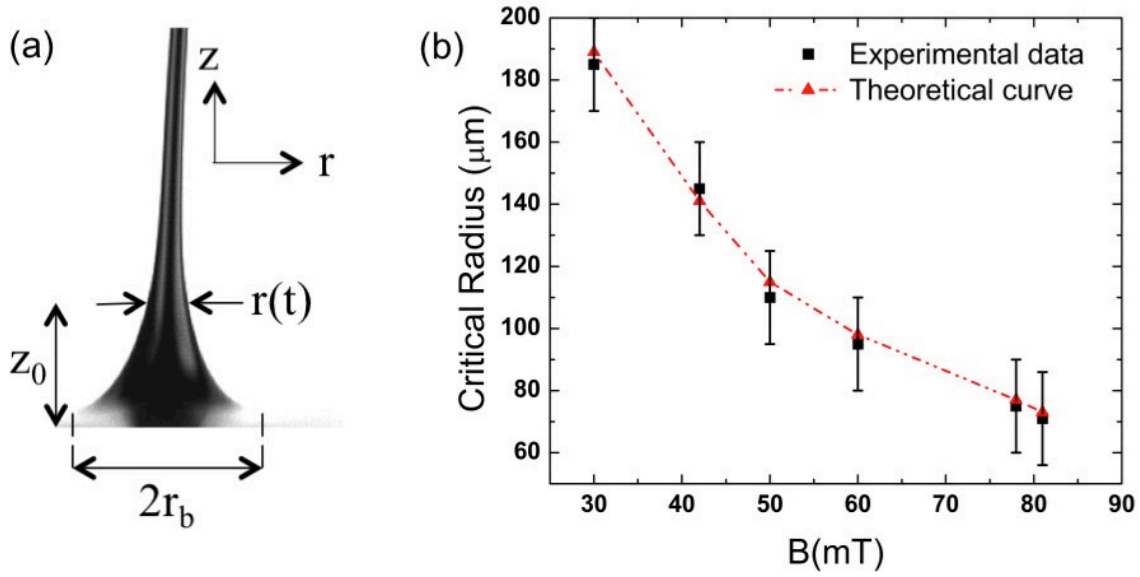

Figure 5. (a) A thinning ferrofluid jet. (b) The predicted critical radii for rupture of the ferrofluid jet are compared with the experimentally measured ones. The membrane for this representative experiment is PCTE membrane with pore size of 5 $\boldsymbol{\mu m}$.

Note that the pressure of the ferrofluid at the base area is equal to the ambient pressure. The boundary condition required to solve Eq. (8) was determined from the experiments. This boundary condition corresponds to the radius of the ferrofluid jet at the rupture coordinate once regime (II) starts. Equation (8) is solved with the Mathematica program and for a representative experiment; $r\,(t)$ is shown in **Fig. 6**. Furthermore, the measured temporal radii of the ferrofluid jet at the rupture coordinate (captured by the high-speed camera) are shown in Fig. 6. Given the functions $r\,(t)$ and r_c, we predicted the time interval of the ferrofluid flow in regime (II), t_2, and consequently dispensed volume in regime (II) through Eq. (3).

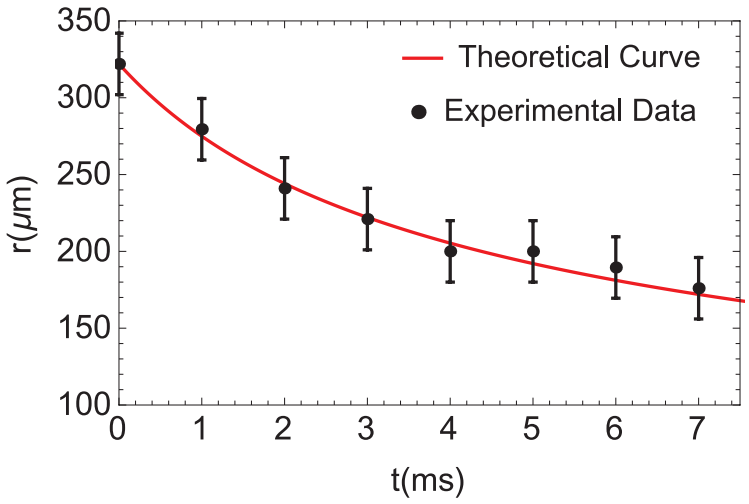

Figure 6. Temporal radius of thinning jet at the rupture coordinate is predicted and compared with the measured radii for the PCTE membrane with the pore size of 5 $\boldsymbol{\mu m}$. The imposed magnetic field in this experiment was 30mT. The agreement between the predictions and the experiments is good for all the experiments.

Summation of the dispensed fluid in regime (I) and regime (II) gives the total dispensed volume of the ferrofluid. The predicted dispensed volumes of the ferrofluid, V_t, are shown in **Fig. 7** for a range of representative membranes. Also, the measured dispensed volumes are included in this figure. The predictions are in good agreement with the measurements. We note that the dispensed volume in regime (II) for all the experiments is less than 20% of the total volume. That is, the major portion of the ferrofluid is dispensed in regime (I).

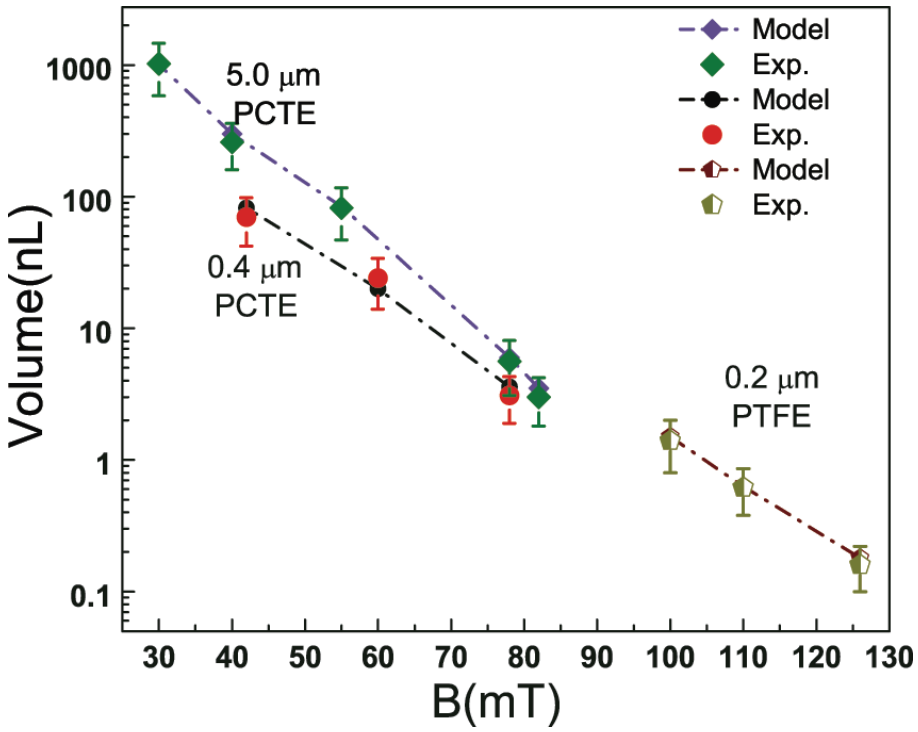

Figure 7. The predicted dispensed volume of the ferrofluid is compared with the measured experimental volumes as a function of the magnetic field at the membrane surface for a range of representative membranes. The dispensed volume can be tuned through hydraulic resistance of the membranes and the magnetic field.

4. Conclusions

In conclusion, we present a facile approach to continuously dispense pico/nano liter volume of the ferrofluid from a ferrofluid reservoir. In this approach, constrained mass flux of the ferrofluid through a membrane, accompanied by an imposed inhomogeneous magnetic field, leads to generation of the ferrofluid droplets in the range of 0.1–1000 nl. Hydraulic resistance of membranes and the magnetic field tunes the dispensed volume and the dispensing frequency.

Furthermore, we developed a model to predict the dispensed volume of the ferrofluid given the properties of the magnetic field, ferrofluid, and the membrane. There is an excellent agreement between the model's predictions and the measurements. The developed approach promises a simple route to dispense the miniature volume of the ferrofluid in biotechnologies, optics, energy systems, and even aerospace technologies without any complex droplet generation devices.[17]

References

1 R. E. Rosensweig, *Ferrohydrodynamics*, Cambridge University Press, England, 1985.

2 I. Torres-Díaz and C. Rinaldi, *Soft Matter*, 2014, 10, 8584–602.

3 P. Irajizad, M. Hasnain, N. Farokhnia and S. M. Sajadi, *Nat. Commun.*, 2016, 7, 1–7.

4 F. N. Pirmoradi, J. K. Jackson, H. M. Burt and M. Chiao, *Lab Chip*, 2011, 11, 3072–3080.

5 A. Jordan, R. Scholz, P. Wust, H. Fähling and Roland Felix, *J. Magn. Magn. Mater.*, 1999, 201, 413–419.

6 K. K. Jain, *Clin. Chem.*, 2007, 53, 2002–2009.

7 G. M. Whitesides, B. a Grzybowski and H. a Stone, *Nature*, 2000, 405, 1033–1036.

8 J. V. I. Timonen, M. Latikka, L. Leibler, R. H. a Ras and O. Ikkala, *Science*, 2013, 341, 253–7.

9 X. Yang, Y. Liu, F. Tian, L. Yuan, Z. Liu, S. Luo and E. Zhao, *Opt. Lett.*, 2012, 37, 2115.

10 J. Tang, S. Pu, S. Dong and L. Luo, *Sensors (Switzerland)*, 2014, 14, 19086–19094.

11 K. Raj, B. Moskowitz and R. Casciari, *J. Magn. Magn. Mater.*, 1995, 149, 174–180.

12 P. Ferraro, S. Coppola, S. Grilli, M. Paturzo and V. Vespini, *Nat. Nanotechnol.*, 2010, 5, 429–435.

13 Y. Wu, T. Fu, Y. Ma and H. Z. Li, *Microfluid. Nanofluidics*, 2014, 9792–9798.

14 P. He, H. Kim, D. Luo, M. Marquez and Z. Cheng, *Appl. Phys. Lett.*, 2010, 96, 10–13.

15 Y. N. Cheung and H. Qiu, *Phys. Rev. E - Stat. Nonlinear, Soft Matter Phys.*, 2011, 84, 1–10.

16 S. S. H. Tsai, I. M. Griffiths, Z. Li, P. Kim and H. a. Stone, *Soft Matter*, 2013, 9, 8600.

17 P. Irajizad, N. Farokhnia and H. Ghasemi, *Appl. Phys. Lett.*, 2015, 107, 191601.